Dynamic reflection interference contrast (RIC-) microscopy : a new method to study surface excitations of cells and to measure membrane bending elastic moduli

A. Zilker, H. Engelhardt, E. Sackmann

J. Physique **48** (1987) 2139-2151 DÉCEMBRE **1987,** PAGE 2139

Classification
Physics Abstracts
87.20

Dynamic reflection interference contrast (RIC-) microscopy : a new method to study surface excitations of cells and to measure membrane bending elastic moduli

A. Zilker, H. Engelhardt and E. Sackmann

Physik Department, Biophysics Laboratory E22, Technische Universität, München, D-8046 Garching, F.R.G.

(*Reçu le 5 juin 1987, révisé le 27 août 1987, accepté le 27 août 1987*)

Résumé. — On présente une nouvelle méthode, la microscopie dynamique par réflexion et contraste interférentiel (RIC), qui permet de mesurer les ondulations thermiques des membranes d'érythrocytes avec une résolution en amplitude inférieure à 50 nm et une résolution en longueur d'onde de 0,5 μm. On analyse la figure d'interférences formée par la lumière réfléchie sur la surface de la cellule interférant avec celle de la lame de verre à laquelle les cellules sont attachées. On propose deux procédures pour l'évaluation de cette figure : d'une part la reconstruction directe du profil instantané de la surface par retransformation de la figure d'interférences RIC, d'autre part l'analyse de Fourier de cette figure d'interférences. Dans la première procédure, le relief créé par les excitations thermiques est obtenu par soustraction de deux profils de surface instantanés ; cette méthode est applicable aux excitations de grande longueur d'onde. Dans la deuxième, on détermine la fréquence spatiale du scintillement par transformée de Fourier de la figure d'interférences RIC. Cette technique est applicable aux excitations de courtes longueurs d'onde ; nous l'utilisons pour déterminer la constante élastique de flexion K_c des excitations de longueurs d'onde comprises entre 0,5 et 1 μm. Cette mesure simultanée de plusieurs valeurs de K_c augmente substantiellement la précision de la mesure. On peut aussi vérifier par cette procédure que les scintillements observés suivent bien la loi d'équipartition. Nous comparons les constantes élastiques des discocytes normaux, des stomatocytes en forme de coupe et des échinocytes. Les valeurs obtenues pour les deux premières classes de cellules sont presque égales : $K_c = 3{,}4 \pm 0{,}8 \times 10^{-20}$ Nm. Les cellules de la troisième catégorie sont beaucoup plus rigides : $K_c = 13 \pm 2 \times 10^{-20}$ Nm. L'avantage principal de la microscopie dynamique RIC est qu'elle permet la mesure des valeurs absolues du déplacement de la membrane qui fait face à la lame de verre, tandis que la spectroscopie de scintillement conventionnelle ne détecte que les fluctuations d'épaisseur de la cellule. L'autre avantage est qu'on peut également l'appliquer aux érythrocytes fantomes et aux autres cellules transparentes.

Abstract. — A new method, the dynamic reflection interference contrast (RIC) microscopy is presented by which thermally excitated surface undulations of erythrocyte plasma membranes — the cell flickering — can be evaluated to an amplitude resolution of $\leqslant 50$ nm and a wavelength resolution of 0.5 μm. The Newtonian interference pattern formed by the interference of light reflected from the cell surface and from the cover glass (to which the cells are slightly fixed) is analysed by a home made fast image processing system. Two evaluation procedures are proposed : firstly the direct reconstruction of the momentaneous surface profile by retransformation of the RIC interference pattern and secondly the Fourier analysis of the interference pattern. In the first case the excitation relief is obtained by subtraction of two momentaneous surface profiles and it is best suited in the long wavelength regime. In the second case the spatial frequency spectrum of the flickering is determined by Fourier transformation of the RIC interference pattern. This technique is reliable in the short wavelength regime and is used here to determine the bending elastic modulus, K_c, in a wave length domain between 0.5 and 1 μm. This simultaneous determination of many K_c-values greatly enhances the accuracy of the measurement. This procedure is also suited to test whether the flickering obeys the equipartition law. The elastic constants of normal discocytes, of cup-shaped stomatocytes and of echinocytes are compared. The values of the first two classes are about equal : $K_c = 3.4 \pm 0.8 \times 10^{-20}$ Nm and agree well with values reported previously [1]. The last cell shape exhibits a substantial higher stiffness $K_c = 13 \pm 2 \times 10^{-20}$ Nm. An outstanding advantage of the dynamic RIC-microscopy is that it allows to measure absolute values of the displacement of the membrane facing the coverslide whereas the conventional flicker spectroscopy [1, 8] can only detect fluctuations of the cell thickness. A second advantage is that it can also be applied to erythrocyte ghosts or to other transparent cells.

1. Introduction.

Plasma membranes of cells belong to the most complex biological systems. Firstly, because its central part, the lipid protein bilayer is a self-organized multicomponent system of lipids and proteins and secondly, because the bilayer is coupled to the glycocalix at the outer side and to the cytoskeleton at the inner side of the cell. In the case of erythrocytes, which are studied in the present work, the cytoskeleton can be considered as a two-dimensional network of coupled entropy springs [2, 3] which is only coupled to the lipid-protein bilayer [4]. Owing to the strong coupling of the three layers, plasma membranes are intrinsic compound systems. That is, any conformational change in one of these three coupled layers will affect the microstructure and the function of the other two lamellae. Thus, at the present stage of membrane research it appears hopeless to study the organization of the membrane or the converted structural changes within its three layers on a molecular level. In such a situation precise measurements of classical phenomenological properties such as viscoelastic parameters or adhesion phenomena are of uttermost interest in order to gain a first insight into microscopic physical properties of the compound membrane and to find structure- function relationships. This point was stressed several years ago by E. Evans [5, 6, 9]. In fact we recently provided evidence that the bending elastic properties are very sensitive to structural changes of erythrocyte membranes caused by variations in the physiological environment of the cell by drugs or diseases [3, 8]. Motivated by such considerations a number of techniques to study mechanical membrane properties have been developed. The most advanced is the micropipette method developed by Evans and coworkers [9] which has been applied to measure elastic and viscoelastic [10] parameters but also thermoelastical properties of natural and artificial membranes.

More recently an electric field jump technique was developed in this laboratory [11] by which creep and relaxation functions of erythrocytes can be measured for very small elongations, that is in the linear range of elongation. Another interesting method is the cell poking [12]. The most precise measurements of the bending elastic properties of plasma membranes or simple lipid bilayers are based on the analysis of thermally excited surface undulations of cells and vesicles. This non invasive technique was first applied to erythrocytes [1, 8] and more recently to vesicles [13, 14]. In the case of erythrocytes the membrane undulations lead to pronounced fluctuation in the brigtness of the phase contrast images, a phenomenon which has been denoted as flickering. Relative values of the bending stiffness are obtained by analysis of the power spectrum of the phase contrast intensity fluctuations in terms of a superposition of Lorentzian lines [1, 8]. This method, called flicker spectroscopy, is very sensitive and simple and enables the detection of subtle changes of the membrane structure [3, 8].

In order to determine absolute values of the bending elastic modulus the absolute amplitudes of the surface undulations have to be measured as a function of the wave vector. This goal was achieved in the case of model membranes by analysing shape fluctuations of flaccid giant vesicles with a fast computer controlled image processing system.

The purpose of the present work is to introduce a new method : the dynamic reflection interference contrast (RIC) microscopy. In combination with a (home made) fast image processing system the membrane excitations can be reconstructed in a dynamic way and the amplitudes can be measured as a function of the wavevector. The method is based on the analysis of the Newtonian-type interference pattern formed by interference of light reflected from the cell surface and the surface of the glass substrate. By direct Fourier analysis of the interference pattern the spatial frequency spectrum of the undulations can be measured with an amplitude resolution better than 50 nm from which the bending elastic constant is obtained in a wavelength region between 0.5 and 1 μm.

2. Physical basis of thermally excited undulations of plasma membranes (Flicker spectroscopy).

The theoretical interpretation of the thermally induced surface excitations of erythrocyte plasma membranes has been given by Brochard and Lennon based on previous work by Kramer [15] and the theory has been extended recently to shape fluctuations of flaccid (non-spherical) lipid bilayer vesicles. Consider for the following summary of the basic idea of the theory a certain piece of the membrane of area S and assume that the x, y-plane of the Cartesian coordinate system is parallel to the plane of the membrane. A given displacement $u(x, y, t)$ in the normal direction is associated with a curvature or bending elastic energy

$$F_B = 1/2\ K_c \int_S [\partial^2 u/\partial x^2 + \partial^2 u/\partial y^2]\, dS \qquad (1)$$

where K_c is the bending elastic modulus. For flaccid cells of biconcave shape the surface tension can be neglected since it contributes only fourth order terms to the elastic free energy [1]. For osmotically swollen cells the surface tension suppresses the bending undulations to very short wavelengths ($\leqslant 100$ Å). Also in cases where a cell is fixed to the glass plate along the whole circumference the surface tension is expected to affect the long wavelength bending modes considerably. Therefore cells which

are only slightly fixed to the substrate were evaluated.

The deformation is associated with two forces acting in the normal direction : firstly a viscoelastic restoring force which is given by the functional derivative of F_B :

$$f_z = K_c[\partial^4 u/\partial x^4 + \partial^4 u/\partial y^4] ; \quad (2)$$

secondly a viscous (or shearing) force arises owing to the hydrodynamic flow in the cytoplasm and the outer medium, respectively, and which is given by

$$\sigma_{zz} = 2\,\eta_c\,\partial u^2(x, y, t)/(\partial t\,\partial z) . \quad (3)$$

Since the viscosity η_c of the cytoplasm is by an order of magnitude larger than that of the (aqueous) outer phase, the latter can be ignored.

If we analyse the displacement $u(x, y, t)$ in terms of a plane wave Fourier expansion

$$U(q) = 1/S \int u(r)\, e^{-iqr}\, d^2r \quad (4)$$

where $q = (q_x^2 + q_y^2)^{1/2}$, the elastic energy may be expressed as a quadratic form

$$F_B = 1/2\, K_c \sum_q q^4\, U(q)^2 \quad (5)$$

and the equipartition theorem may be applied. Therefore a value of the curvature elastic modulus, K_c, may be determined from the mean square amplitude of each mode of wavevector q according to

$$K_c = k_B\, T/(Sq^4 \langle |U(q)|^2 \rangle) \quad (6)$$

where S is the observed surface.

Each mode is further characterized by a relaxation time [1] :

$$\tau_q = 4\,\pi\eta_c/(K_c\, q^3) . \quad (7)$$

In the above consideration the constraints of the surface excitations owing to the finite size of the cell and any coupling between the excitations of the two opposing membranes of the red blood cell have been ignored. This is possible for modes with wavelengths $\lambda = 2\,\pi/q$ which are small compared to the diameter, L, of the cell (which holds for $\lambda \leqslant 1$ μm). Since the present technique is restricted to this regime of modes the above approximation is sufficient.

It should be noted that the expansion of the surface excitations in terms of plane waves becomes a poor approach in cases where extended membrane regions are fixed to the substrate.

3. Principle of dynamic reflection interference contrast (RIC) microscopy of surface undulations.

The reflection interference contrast microscopy turned out to be a powerful technique to study the interaction of cells with surfaces [16, 17]. However, its inherent strength to study the dynamic cellular processes has to our knowledge not been recognized yet.

The principle of the RIC-technique is depicted in figure 1. The light reflected from the glass surface (called reference beam in the following) and that reflected from the cell surface (called object beam) are brought to interference. If the object is a cell exhibiting cylindrical symmetry as assumed in figure 1, the RIC micrograph exhibits a series of concentric Newtonian rings as shown in figure 2a and 2b. It is clear that the surface profile of the object can be reconstructed from the RIC-interference pattern.

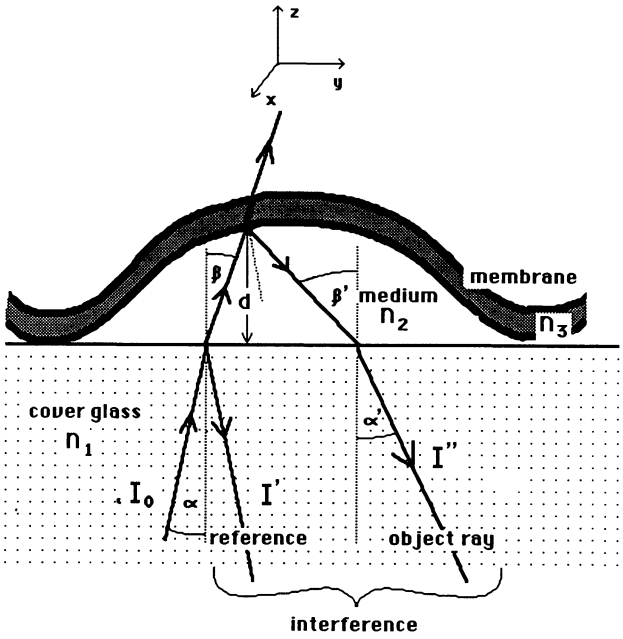

Fig. 1. — Schematic representation of reflection interference contrast (RIC) microscopy of the surface of a cell (case of erythrocyte). k_0 and I_0 are the wave vector and the intensity of the incident light, respectively. k' and I' are the corresponding values of the light reflected from the glass plate (called reference beam), k'' and I'' those of the light reflected from the cell surface, called the object beam.

One main advantage of the RIC-technique is that it can also be applied to transpaent cells such as erythrocyte ghosts (cf. Fig. 2d). In order to allow perifusion and to avoid transversal and lateral motion of the whole cells they are slightly fixed to the glass surface by polylysine. Figure 3 illustrates how the cell flickering is manifested in the RIC-diffraction pattern. It is demonstrated how the Newtonian rings are fluctuating in a lateral direction owing to the thermally excited deformations of the membrane. For three cases the Fourier amplitude spectra

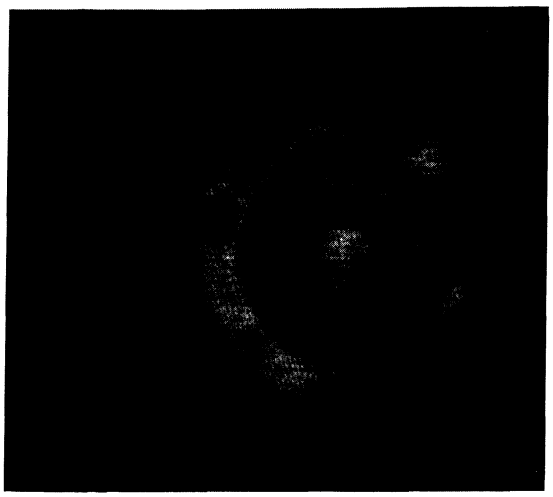

2(a)

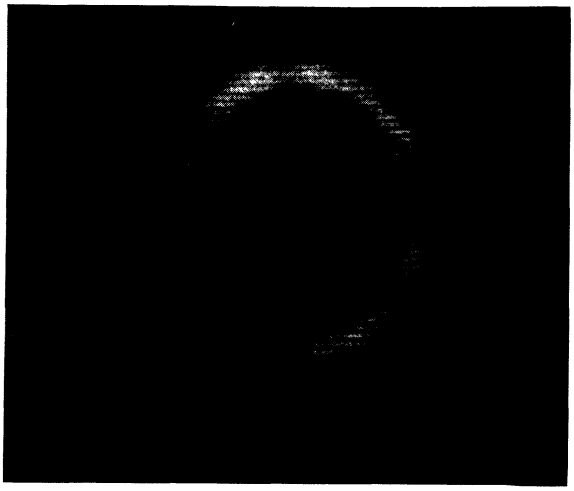

2(b)

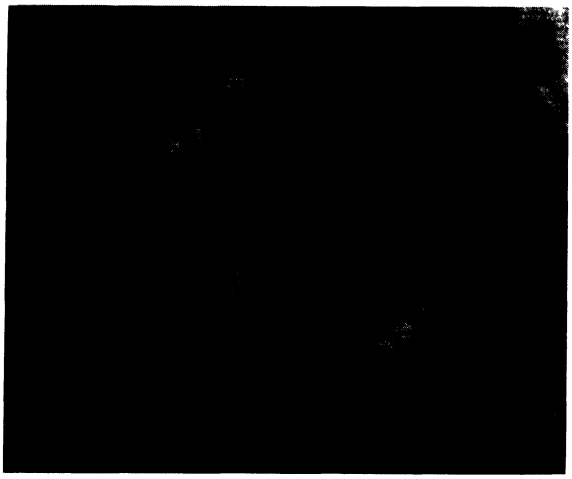

2(c)

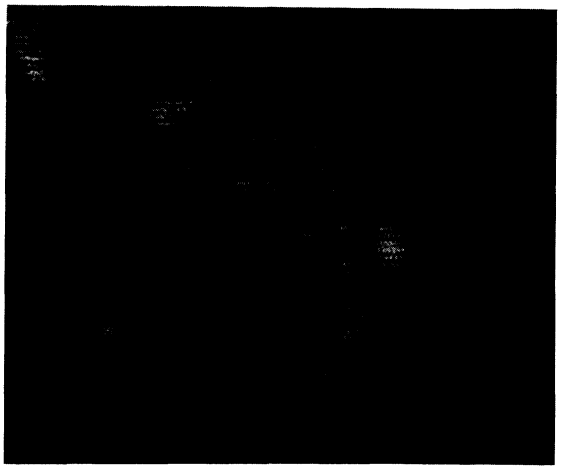

2(d)

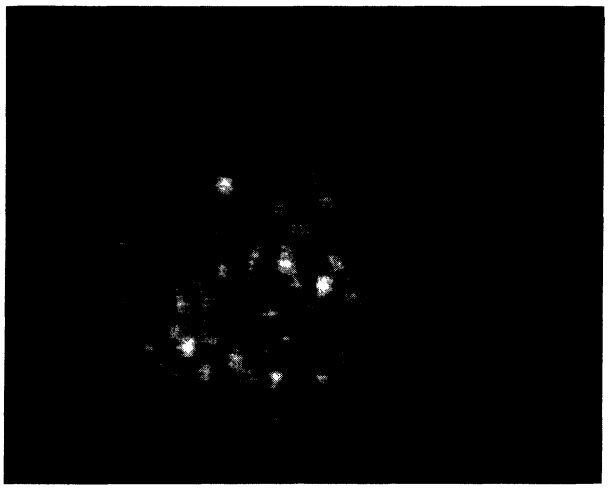

2(e)

Fig. 2. — Typical RIC-images of erythrocytes slightly fixed to a glass-slide exhibiting characteristic cellular shapes : a) normal discocyte b) cup shaped stomatocyte viewed in direction of invagination c) echinocyte. The regions of the cell surface which are attached to the glass appear black. Figure 2d shows a RIC-micrograph of a ghost. Figure 2e shows the RIC-micrograph of a lymphocyte.

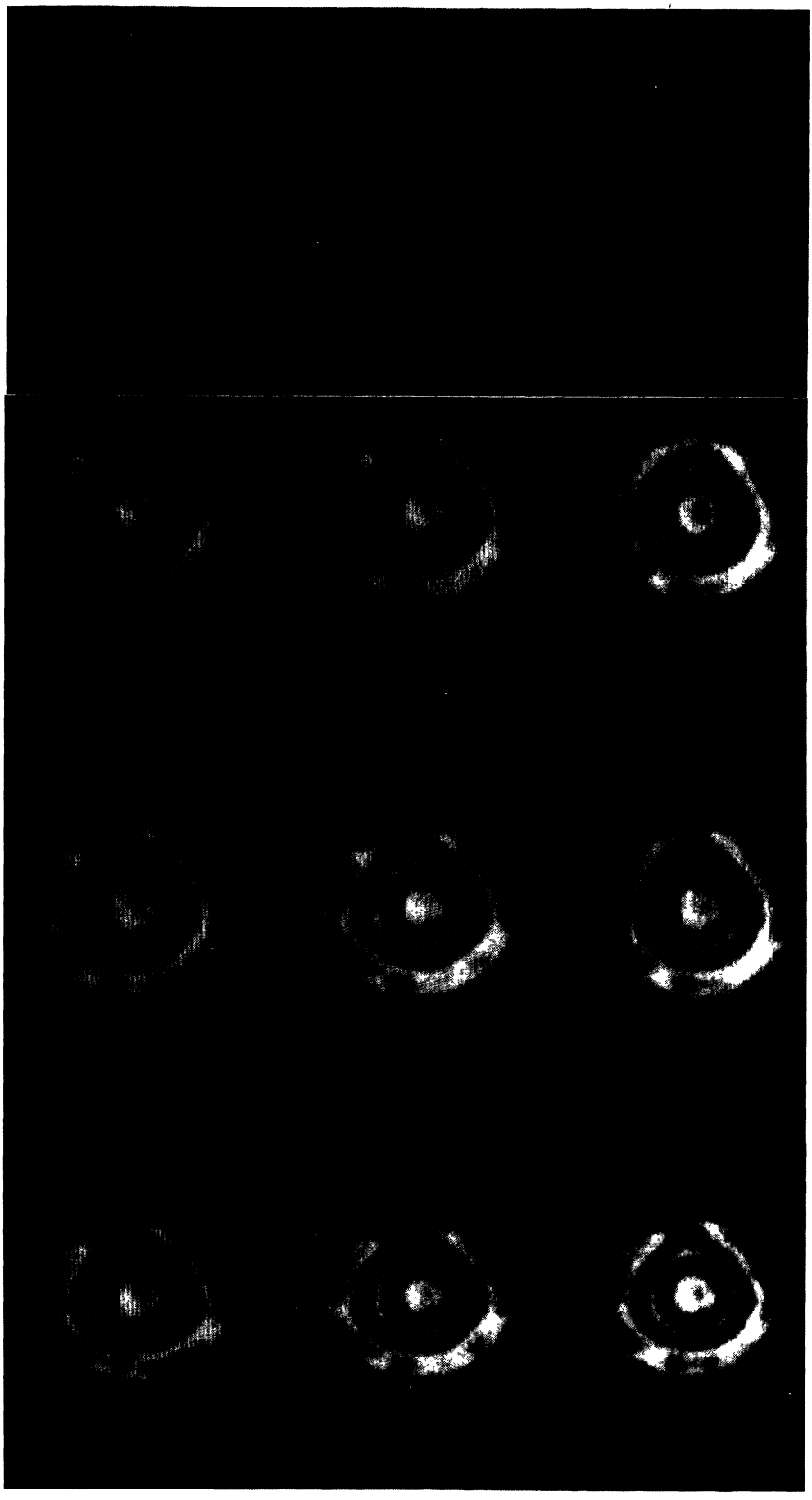

Fig. 3. — RIC-micrograph of a biconcave erythrocyte taken at subsequent time intervals of 0.2 s which shows the time dependent lateral deformations of the Newtonian rings. On the right side the Fourier transform of the interference pattern is given for three samples. The fluctuations caused by the flickering are clearly visible also in the Fourier transform.

of the RIC-pattern are shown simultaneously with the latter. Also in this case the time dependent fluctuations of the positions and intensities of the Fourier amplitudes particular at large spatial frequencies are clearly visible.

From the technical point of view, the main problem is to separare the RIC-pattern from the very strong background caused by the reflection (of the incident light) at the objective lenses and by stray light. For normal incidence (aperture angle $\alpha = 0$ in Fig. 1) the intensities of the object and the reference beams are

$$I' = I_0(1 - R_1) \quad \text{and} \quad I'' = I_0(1 - R_1)\, R_2 \quad (8)$$

where

$$R_1 = ((n_1 - n_2)^2/(n_1 + n_2)^2)^2$$

and

$$R_2 = ((n_2 - n_3)^2/(n_2 + n_3)^2)^2$$

are the reflectivities of the glass and the cell surfaces ; respectively. For $n_1 = 1.51$, $n_2 = 1.33$ and $n_3 = 1.4$ (cf. Fig. 1 for definition of refractive indices) it is $I' \approx 4 \times 10^{-3}\, I_0$ and $I'' \approx 6.5 \times 10^{-4}\, I_0$, that is the RIC-intensity is very weak compared to the background. The problem is overcome by the so-called Antiflex-technique [18]. The light which is reflected by the lens surfaces is eliminated by a $\lambda/4$ wave plate placed between the object and the objective lens and crossed polarizers in the illumination and observation path of light.

Consider now the correlation between the intensity distribution $I(x, y, t)$ of the RIC-diffraction pattern and the surface profile as characterized by the distance $d(x, y, t)$ between the surface of the glass plate and the cell (cf. Fig. 1). It is generated by the superposition of the plane waves of the reference beam E' and the object beam E''.

As a first approximation we consider normal incidence of the illumination ligth that is its wave vector k_0 is parallel to the z-axis. This is justified for the following reason : according to Gingell and Todd [19] it is essential to work at small numerical apertures in order to minimize errors caused by a reduction of the contrast of the higher order Newtonian rings and shifts of the positions of the rings. In our case the objective serves as a condensor and the maximum angle between k_0 and the z-axis is $\alpha = 31°$. For such an angle the errors are smaller than 10 % and the assumption of normal incidence is acceptable. The maximum lateral resolution is 0.5 μm.

For normal incidence with $k = k_0\, n_2$ the reference and object waves are

$$E'(x, y, t) = E_0' \exp^{i(\omega t + 2kz(x, y))} \quad (9a)$$

$$E''(x, y, t) = E_0'' \exp^{i(\omega t + 2k(z(x, y) + d(x, y, t)))}. \quad (9b)$$

Superposition of the two waves at the position $z(x, y) = 0$ leads to the following intensity distribution

$$I(x, y, t) = A' + 1/2\, A'' \cos 2kd\,(x, y, t) \quad (10)$$

with

$$A' = E_0'^2 + E_0''^2 ; \quad A'' = E_0'\, E_0'' . \quad (11)$$

Note that the beam reflected at the cell surface suffers a phase shift of 180°.

4. Instrumentation, cell preparation and image processing.

4.1 THE MICROSCOPE. — The RIC micrographs are taken with a Zeiss Axiomat inverted microscope equipped with an antiflex oil immersion objective (Antiflex Neofluar 63/1.25). Illumination is performed with a high pressure Hg-lamp (Osram HBO 100 W) and monochromatic light of $\lambda = 546$ nm is produced by a combination of an interference and a cut-off filter (Schott A3-546 and OG 530).

The use of an oil immersion objective is essential for the RIC microscopy in order to eliminate the strong reflection at the air-to-cover glass interface which would completely superimpose the RIC-image. As noted above the correspondence between the RIC-pattern and the surface profile of the cell gets worse with increasing numerical aperture of the objective. The effective numerical aperture of the antiflex objective is 0.75 which corresponds to a resolution of 500 nm and the error in the reconstruction of the surface profile resulting from those restrictions is only about 10 %.

4.2 CELL PREPARATION. — Blood is drawn from finger tips or arm veins and is diluted with NaCl-ACD buffer at a ratio of 1 : 4. The erythrocytes are separated from the other blood cells by centrifugation (5 min at 2 000 g) and taken up in buffer at a hematocrit of 50 %. For the measurement this cell suspension is further diluted by addition of a 400 fold excess of buffer. Immediately after the transfer to the buffer about 95 % of the cells are transformed to stomatocytes. Three hours after incubation at 37 °C or 12 h at 25 °C about 70 % of the cells regenerate to discocytes.

For the microscopic observation the cells are brought into a home made flow chamber which was described and which enables perifusion of the cells during the measurement [8]. The observation window is a cover glass of 0.017 cm thickness and the cells are slightly fixed to its surface. For that purpose the glass surface is covered with polylysine of molecular weight 1 500 as described previously [8]. By using a low molecular weight polycation a too strong attachment of the cells to the surface is avoided which would affect the undulations of the membrane adjacent to the glass surface. Erythrocyte

ghosts are prepared by perifusion of the prefixed cells with millipore water until hemolysis occurs whereupon the chamber is perfused with the buffer again.

4.3 IMAGE PROCESSING SYSTEM AND DATA HANDLING. — The data acquisition and processing system consists of the following parts :

1) A CCD camera purchased from Aqua-TV (8960 Kempten, Germany) equipped with a Thomson THX 31133 sensor : a CCD (= charge coupled device) chip. It comprises 384 horizontal and 288 vertical picture elements each with an area of $23 \times 23\ \mu m^2$ so that the total image size is 0.66×0.88 cm. The frame transfer rate is 25 per second, that is the read-out time for a complete image is 40 ms.

2) A Sony U-Matic video recorder (VO 5800 PS) which is coupled to the CCD-camera for recording the images during the measurement. For further image processing the images from the recorder are divided into 512×512 pixels and the brightness into 256 gray levels.

3) The home made image processing system conceived and constructed by H. Engelhardt and H. P. Duwe consist of the following subunits : (i) A central processing unit of the KWS company (7505 Ettlingen, Germany) based on a 16 bit Motorola 68000 processor. (ii) The image storage memory is $512 \times 512 \times 8$ bit deep thus allowing 256 gray levels.

4) The digitized images are displayed on a videomonitor (Blaupunkt, HRCD 37-121 RGB) *via* a digital-to-analog converter.

5. Evaluation of surface undulations of membranes.

A direct and rigorous reconstruction of the time dependent surface profile from the RIC pattern by inversion of equation (10) is not possible because the background intensity A' and the contrast factor A'' may vary significantly over the field of interest in the microscopic picture. Standard surface reconstruction methods like phase shift interferometry [20], where the phase $\varphi_r = 2\,kz(x, y)$ of the reference beam is altered with respect to the object beam, are not applicable because of the optical set-up and the small distance between cell and cover glass ($d \approx 1\ \mu m$). In the present work two new aproximation procedures are applied.

The first consists in a direct reconstruction of the momentaneous surface profile taking into account the fundamental shape of the cell. The spatial inhomogeneities in the background intensity are eliminated and a contrast correction is performed as will be described below.

The second method consists of a direct Fourier analysis of the RIC-diffraction pattern. The spatial correlation function is obtained by approximate solution of equation (4) and the mean square amplitudes $\langle U(q)^2 \rangle$ (and thus the bending elastic modulus) can be determined as a function of the undulation wave vector.

5.1 SURFACE RECONSTRUCTION TECHNIQUE. — The method is based on the evaluation of the inverted equation (10).

$$\varphi_0 = 2\,kd(x, y, t) = \arccos\,(2(I - A')/A'') \,. \quad (12)$$

The intensity distribution $I(x, y, t)$ at a given time is stored in the form of a 128×128 matrix $I(m, n)$. The magnification factor of the microscope is set in a way that the RIC image of the cell fits neatly into the frame (cf. Fig. 3). For processing the cell is divided into small sections through the cell centre in the radial direction. The radii are approximated in the discrete lattice by using the Bresenham plotter algorithm [21]. The number of extrema along the sections is compared to the number of Newtonian rings of the RIC-image of the cell in order to eliminate spurious extrema caused by dust on the cover glass or local defects of the CCD camera. Further processing of the radial intensity distribution is performed in three steps as illustrated in figure 4a.

Step 1 : ($1 \rightarrow 2$ in Fig. 4a). The background intensity A' is implicitly subtracted by considering only the relative differences $(I_{max} - I_{min})$ between the subsequent extrema within one half cycle of the cosine-interference function. It should be noted that the value of $(I_{max} - I_{min})$ varies across the cell since the local contrast transfer function is determined by the slope of the cell surface. $(I_{max} - I_{min})$ is averaged over all intensity extrema along the cross section. The extrema on both sides of the centre are expanded to the full range of the cosine function given by equation (13) with linear interpolation within each successive half period. The depth of the central dip needs special consideration because there the interference function does not reach its extreme values. In the present approach it is scaled with the average $\langle I_{max} - I_{min} \rangle$.

$$\cos\,\varphi(r, t) = \cos\,2\,kd(r, t) = (2(I(r, t) - I_{min})/ /(I_{max} - I_{min})) \quad (13)$$

Step 2 : ($2 \rightarrow 3$ in Fig. 4a). The calculation of arccos φ from equation (13) leads to discontinuities at $\varphi = 0, 2\,\pi \ldots$ However, since the cell shape of a discocyte is known, the segments of $\varphi(r, t)$ are assembled to a continuous function.

Step 3 : ($3 \rightarrow 4$ in Fig. 4a). Since the cell symmetry has been ignored until now, curve (3) is a monotonously ascending function. The form of the discocyte is easily obtained by flipping curve (3) at appropriate points leading to curve (4).

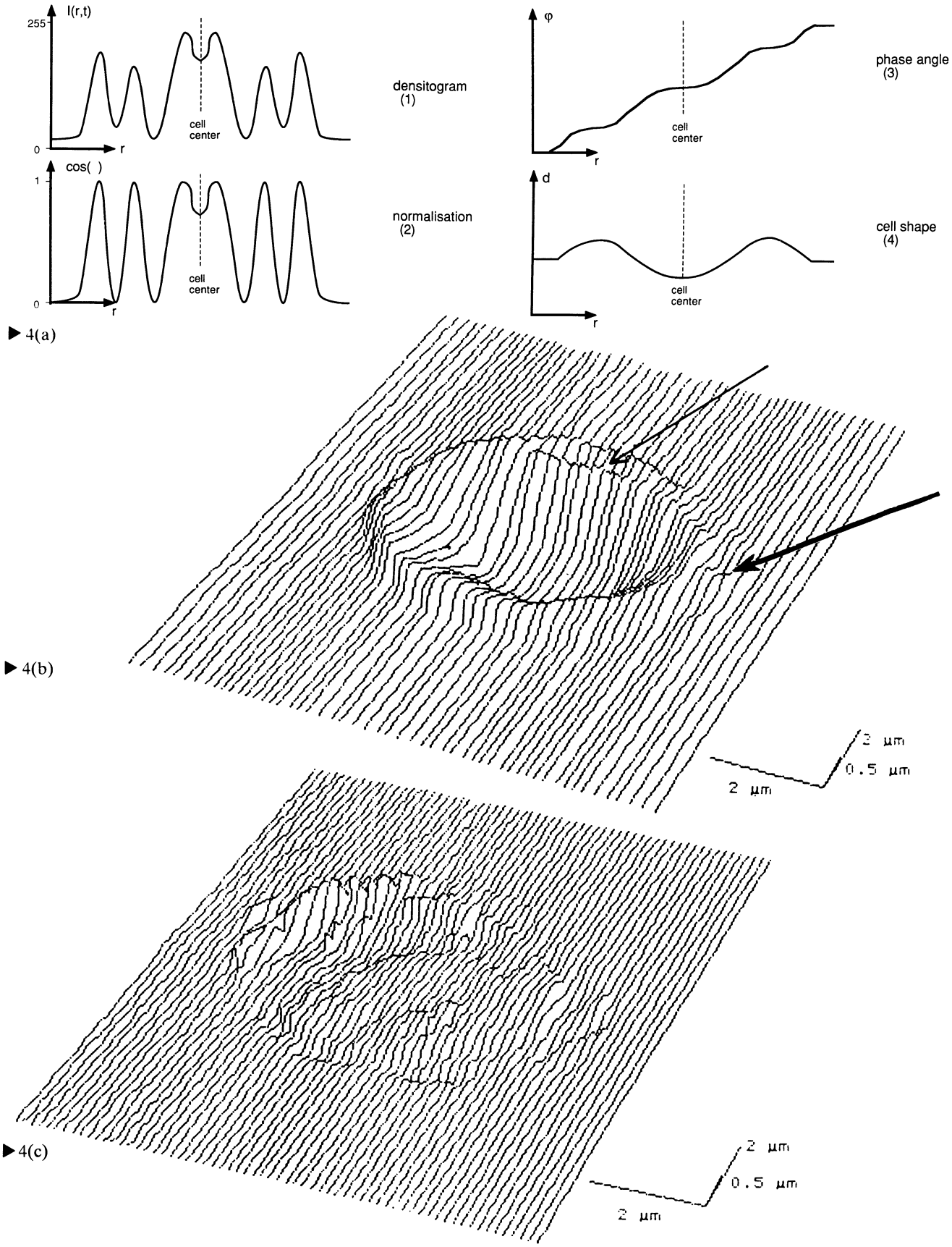

Fig. 4. — Demonstration of the direct reconstruction of a membrane surface. a) Curve (1) represents the intensity distribution of RIC-pattern along a section through centre of cell. Curve (2) is obtained by normalization of the maxima and minima of curve (1). Curve (3) is the inverse function of curve (2) assembled to a continuous form. Curve (4) represents the cell profile. b) Perspective representation of cell surface as reconstructed by the above procedure. The sharp edge indicated by a thin arrow corresponds to an area where the cell is fixed to the cover glass. The spikes indicated by a thick arrow are caused by a dust particle. c) Momentaneous image of surface excitations of an erythrocyte as obtained by subtraction of two momentaneous surface profiles.

The above procedure is performed for each section through the centre and these sections are then put together in a continuous way.

Figures 4b and c show examples of application of the surface reconstruction technique. The surface of a red blood cell is presented in perspective.

Clearly the concave shape of the discocyte is faithfully reproduced. The momentaneous excitations of the cell surface can be generated (at time intervals larger than 0.04 s) by subtraction of two momentaneous surface profiles. An example is shown in figure 4c. A severe drawback of this image reconstruction technique is its high sensitivity to deviations of the interference pattern from the rotational symmetry which is essential for computerized analysis of the fringes.

5.2 FOURIER ANALYSIS OF RIC-INTERFERENCE PATTERN. — The above reconstruction method is well suited for visual presentation of the long-wavelength excitations. The following method based on the Fourier analysis of the RIC-pattern becomes most powerful for the small wavelength domain and allows a direct determination of K_c.

Since we are interested to apply the RIC technique to detect the transient excitations of the membrane we decompose the distance $d(x, y, t)$ into a time independent part $d_0(x, y)$ and a fluctuating part $u(x, y, t)$.

$$d(x, y, t) = d_0(x, y) + u(x, y, t) . \quad (14)$$

The flicker amplitude $u(x, y, t)$ is determined by the following approximate evaluation procedure.

By application of the addition theorem, the expression cos $(2\,kd)$ in equation (10) is split into two terms : one proportional to cos $(2\,ku)$ and the other to sin $(2\,ku)$. The flicker amplitudes $u(x, y, t)$ are of the order of $u < 0.1$ μm and are thus small compared to the wavelength of light ($\lambda_L = 0.546$ μm). We therefore introduce the approximation

$$\cos\,(2\,ku) \approx 1 \quad \text{and} \quad \sin\,(2\,ku) \approx 2\,ku$$

so that

$$I(x, y, t) \approx A' + 1/2\,A'' \cos 2\,kd_0(x, y) + \\ + kA''\,u(x, y, t) \sin 2\,kd_0(x, y) . \quad (15a)$$

By introducing the time averaged RIC intensity distribution

$$\langle I(x, y, t)\rangle_t = A' + 1/2\,A'' \cos 2\,kd_0(x, y) \quad (15b)$$

calculated from 16 subsequently recorded RIC-images of the cell and subtracting it from (15a) it follows :

$$u(x, y, t) \sin 2\,kd_0(x, y) = \\ = (I(x, y, t) - \langle I(x, y, t)\rangle_t)/kA'' . \quad (15c)$$

The next aim is to determine the spatial Fourier transformation of the momentaneous flicker amplitudes $u(x, y, t)$ from which the curvature elastic modulus K_c is obtained according to equation (6). Consider for that purpose the Fourier transformation of the left side of equation (15c)

$$I(q) = \int u(r, t) \sin\,(2\,kd_0(r))\, e^{-iqr}\, d^2r \quad (16)$$

where r is the radius vector in the x, y-plane.

According to the convolution theorem, $I(q)$ is the convolution of the Fourier transformations of the flicker amplitude $u(r, t)$ and the sine function, respectively. The former is

$$FT\{u(r)\} = U(q) = 1/S \int u(r)\, e^{-iqr}\, d^2r . \quad (17)$$

A rigorous deconvolution of the two partially overlapping transformations is not possible [22]. Fortunately the resting shape $d_0(x, y)$ for a normal discocyte cell is a slowly varying function and thus the Fourier transformation

$$D_0 = FT\{\sin\,(2\,kd_0(x, y))\}$$

is bandwidth limited around $q = 0$. In a first, coarse approximation D_0 can be replaced by a δ-function at $q = 0$. So the convolution with D_0 reproduces the desired function $U(q)$ [23]. The applicability of this approximation procedure for excitation wavelength $\lambda = 2\,\pi/q < 1$ μm is demonstrated below (Sect. 6).

A second problem to be solved arises from the fact that the fluctuations in the intensity caused by the flickering is modulated by the interference pattern of the resting form and that the amplitudes of these oscillations vary along the sections through the cell as in figure 4a. The degree of modulation is proportional to the slope of the interference pattern of the resting form. We solve this problem by multiplying the intensity fluctuation associated with the flicker amplitudes with the average slope $2/\pi$ of the sinusoidal variation of the intensity $I(x, y)$ caused by the resting form. With this approximation one obtains

$$U(q) = I(q)\,\lambda/(2\,A'') . \quad (18)$$

Since $A'' \approx I_{max} - I_{min}$ varies along the sections through the cell an average value obtained from the 3-dim. reconstruction is used. Inhomogeneities of the background illumination contribute only to the wave vector domain around $q \approx 0$ and can therefore be neglected in this approximation. In figure 5 we present as examples the spatial frequency spectra $U(q)$ of the flicker amplitude for a normal erythrocyte (a) and a cup-shaped cell (b). The spectra are superpositions of a sharp band with a maximum at about 4 μm and a broad band which extends to

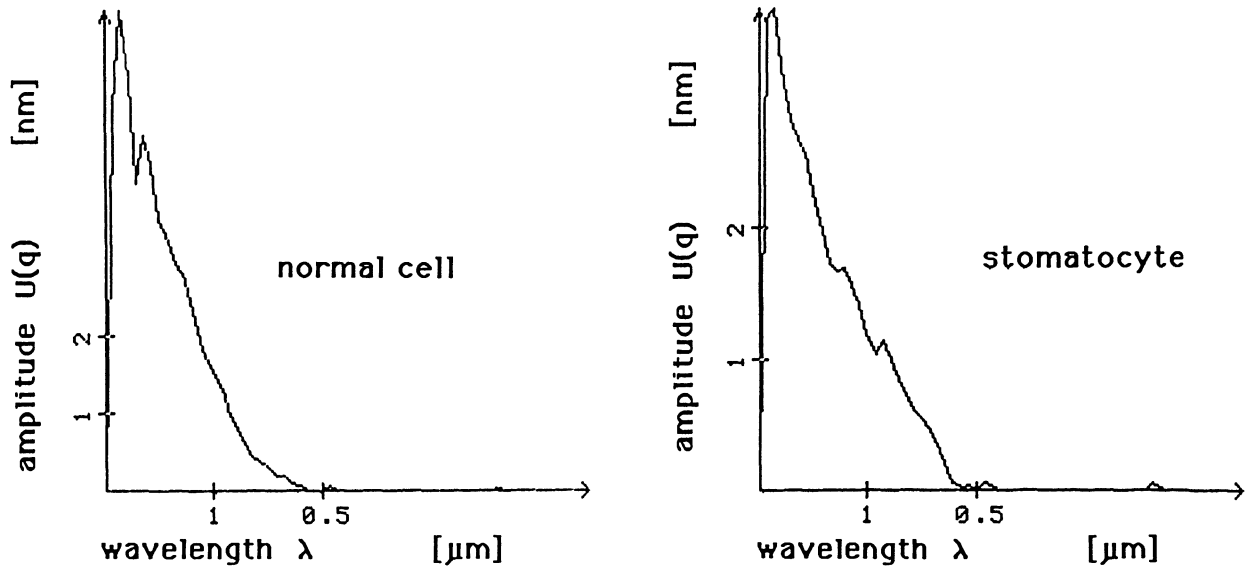

Fig. 5. — Examples of Fourier transformed flicker amplitude $U(q)$ for normal biconcave erythrocyte (left side) and for cup-shaped cell (right side).

$\lambda \approx 0.5$ μm. The former corresponds to the spectrum of the resting state and the latter to that of the undulations. As expected the width of the resting state spectrum is much larger for the cup shaped cell than for the discocyte. The parameter S in equation (6) represents the area of the flickering part of the cell. It is measured directly from the video screen by calibration with a gauge cover slide.

6. Application of RIC-flicker spectroscopy.

In the following the Fourier transform technique is applied to measure the bending elastic constants of normal and transformed erythrocytes.

According to equation (6) the bending elastic modulus K_c is directly obtained from the mean square amplitude of the spatial frequency spectrum of the flicker amplitude. The latter is obtained by averaging first over 16 two dimensional $U(q_x, q_y)$-spectra and then over the azimuth angle in the q_x, q_y-plane. The modes are correlated if the time interval between two samples is smaller than the relaxation time of the longest wavelength mode. For that reason we varied the sampling time until correlations between subsequent images are negligible which holds for sampling times greater than 0.2 s. This value was chosen for the following experiments. In figure 6 the product $\langle U^2 \rangle\, q^4$ for three different cells of three different donors are plotted (on a logarithmic scale) as a function of the wave vector q. According to equation (6) this is a measure of K_c and should not depend on q. K_c is indeed constant between 0.5 and 1 μm but increases strongly for longer wavelengths, λ, and more slowly for $\lambda < 0.5$ μm.

The increase at shorter wavelengths is partially

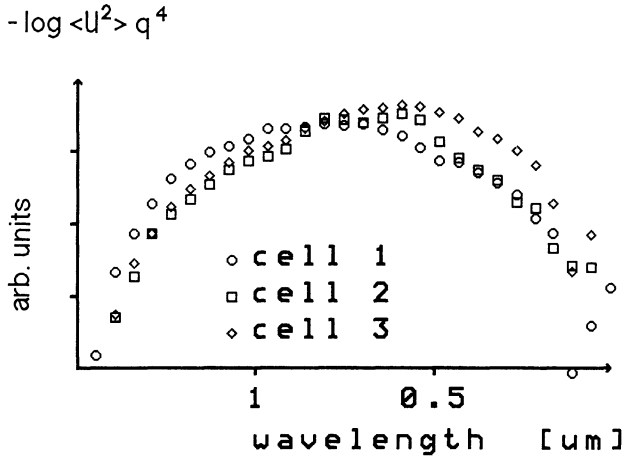

Fig. 6. — Plot of logarithm $\langle U^2 \rangle\, q^4$, as function of wavelength $\lambda = 2\pi/q$ for three cells of different donors from which K_c can be obtained according to equation (6).

due to the finite sampling time of the CCD camera. According to equation (7) the relaxation time, τ_q, decreases very strongly with increasing q-vectors and thus becomes smaller than the video sampling time ($\tau_{sam} = 1/25$ s) below 0.5 μm. A possibly more important reason is a truncation of the short wavelength modes by the low-pass filtering owing to the width of the aperture which restricts the spatial resolution to about 0.5 μm. The strong increase of K_c for excitation wavelengths larger than 1 μm is a consequence of the coupling of spectra of the resting form and the undulations.

It thus follows that at the present stage of the technique reliable values of K_c are only obtained in the finite region of excitation wavelengths: $0.5\ \mu m < \lambda < 1\ \mu m$. On the other side with the

present Fourier transform technique, K_c, is simultaneously measured many times corresponding to a drastic increase in the accuracy of the measurement. The constant value of K_c at $0.5\ \mu m < \lambda < 1\ \mu m$ provides strong evidence that the flickering is a thermally excited process and that all modes are equivalent at least in this wavelength region.

The average values of the elastic constants of the three cells agree very well : $K_c = 3.4 \pm 0.8 \times 10^{-20}$ Nm and this value lies within the range reported by Brochard and Lennon [1] : $K_c = 2 - 7 \times 10^{-20}$ Nm.

In figure 7 the elastic constants of two pathological cell shapes are compared : whereas the elastic modulus of $K_c = 4.2 \times 10^{-20}$ Nm (between 0.5 and 1 μm) for the cup shaped cell agrees well with the value of discocytes the echinocyte exhibits a considerably higher bending stiffness : $K_c = 13 \pm 2.5 \times 10^{-20}$ Nm. The substantial increase of K_c above about 0.75 μm is a consequence of the strong spatial variation of the profile of the resting state of echinocytes. In the experiment the elasic constant is mainly measured between the spiculi. The higher bending resistance could be due to a higher protein density of these membrane regions as is suggested by freeze fracture experiments.

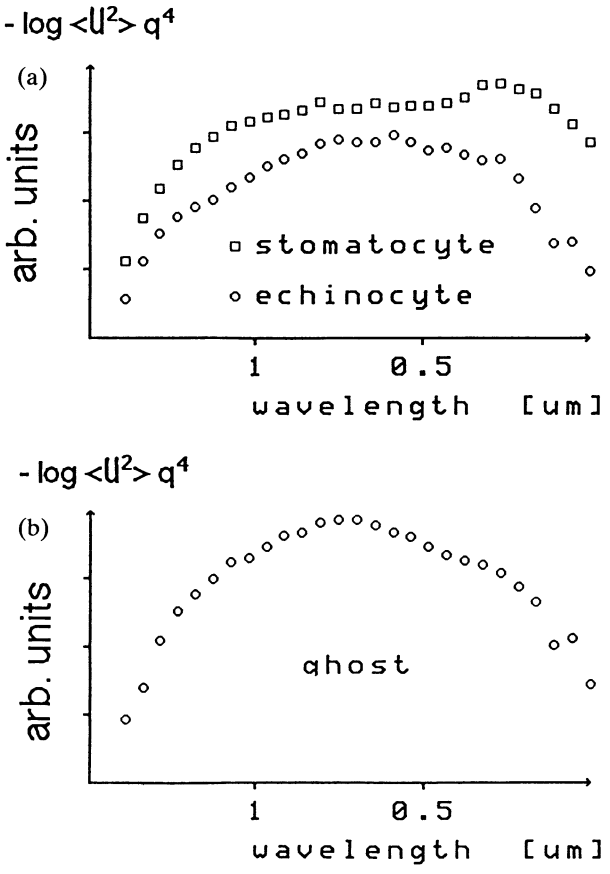

Fig. 7. — a) Comparison of log $\langle U^2 \rangle\ q^4$ plot for two shape transformed cells : a stomatocyte (□) and an echinocyte (○). b) log $\langle U^2 \rangle\ q^4$ plot of a ghost.

Figure 7b shows a measurement of an erythrocyte ghost. A slightly smaller elastic modulus ($K_c = 1.5 \times 10^{-20}$ Nm) is found than for normal cells. The experiments of figure 7 show that the bending elastic constant is very sensitive against structural changes of the plasma membrane. Ample experimental evidence for this was found in a recent study of the erythrocyte flickering by the dynamic flicker spectroscopy.

7. Concluding discussion.

Although at the present state a number of severe approximations had to be introduced, the dynamic RIC microscopy provides a powerful tool for the precise measurement of bending elastic constants K_c of erythrocyte plasma membranes because it allows to measure absolute displacements of the cell membrane. The absolute bending modulus K_c as measured by the spatial Fourier transform spectroscopy of the interference pattern agrees well with values obtained by the phase contrast microscopy. The main advantage of this method is the very high resolution of the flicker amplitudes of better than 50 nm and the possibility to measure K_c simultaneously for a whole range of wave vectors q. Although this range is limited to $0.5\ \mu m < \lambda < 1\ \mu m$ the sensitivity and precision of the elastic constant measurement is drastically improved in this way. Moreover it is also possible to find out whether certain modes are preferred. As judged from the present experiments the equipartition law holds for the erythrocyte flickering at least up to wavelengths of about 1 μm.

At long wavelengths the constraints of the cell geometry are expected to come into play. This problem could be studied with the second method of evaluation, the dynamic reconstruction of the cell surface profile which is best suited in order to evaluate the long wavelength excitations but provides poor results in the regime of large q-vectors. This method has not been fully exploited in the present work.

A further prominent advantage of the RIC technique is that it can also be applied to study erythrocyte ghosts or any other transparent cells. In fact, the dynamic reconstruction version should be excellently suited to study membrane deformation associated with cell locomotions or other large scale membrane deformations such as pseudopodia formation.

A severe problem of the present Fourier transform technique is the mixing of the flickering modes by the resting form of the cells. We do not yet see an easy solution to this problem of deconvolution of the resting form and the undulations.

Another problem is the high light intensity required for the RIC-microscopy which implies the

danger of a photochemically induced denaturation of proteins. This effect is demonstrated in figure 8 where the effect of a prolonged illumination of the cell on the excitations is drastically demonstrated. The surface undulations are nearly completely suppressed after about three minutes of exposure. The following experiment provides evidence that this reduction in the flickering is caused by the photochemically induced polymerization of hemoglobin : if a normal cell is opened by osmotic shock the hemoglobin flows out rapidly (Fig. 8d left). After prolonged illumination the leakage is much slower and the outflowing hemoglobin is lumped together (cf. Fig. 8d right). The problem is overcome by using monochromatic light and by the high optical quality of the Axiomat microscope.

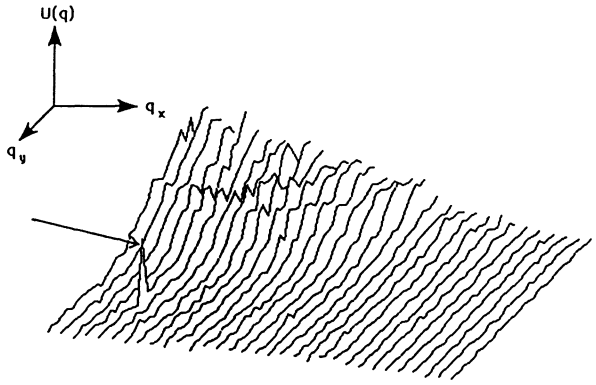

8(a)

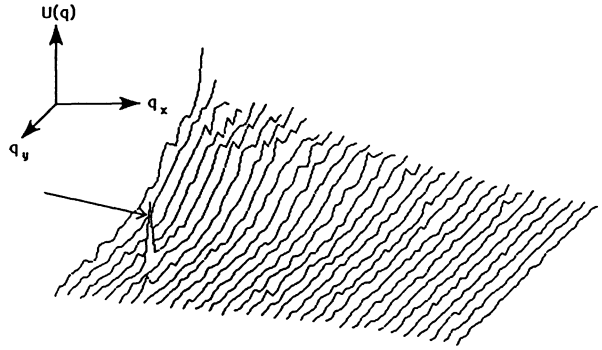

8(b)

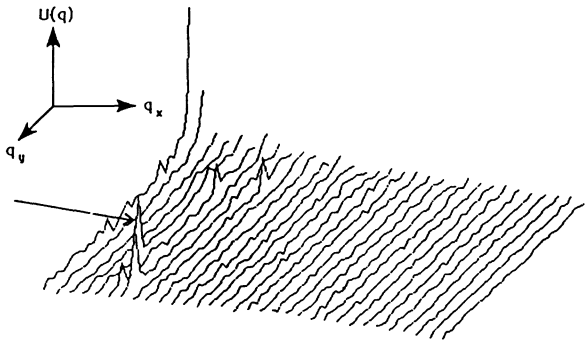

8(c)

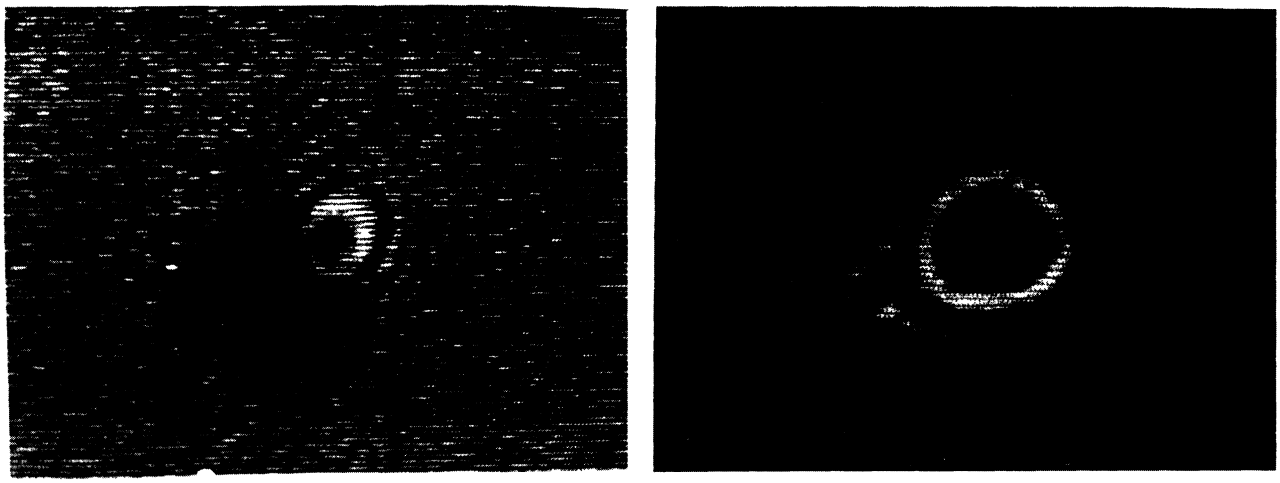

8(d)

Fig. 8. — Effect of strong illumination on the spatial flicker spectrum of erythrocytes after (a) 0 s, (b) 85 s and (c) 165 s of illumination with unfiltered light. The spatial frequency spectrum $U(q)$ is plotted in the q_x, q_y-plane. The spikes indicated by arrows are caused by the CCD-camera. Figure 8d shows on the left the leakage of hemoglobin from a normal cell after osmotic shock and on the right the same process after 90 s of illumination. Note that the hemoglobin is lumped together in the second case.

An intriguing question is whether the flickering of erythrocytes is only an interesting physical effect or if it fulfils some biological purposes. There are at least two examples how nature could exploit the flickering : the first one is an improved mixing of the cytoplasm by the hydrodynamic flow associated with the membrane excitation which would accelerate the oxygen exchange ; the second one is the hindrance of the adhesion of the red blood cells to the walls of capillaries or to the surface of other tissue by non-specific forces. It has first been postulated by Helfrich [24] that the surface undulation of membranes can contribute considerably to the steric repulsion of vesicles or cells and very strong experimental evidence for this hypothesis has been provided by Evans and Parsegian [25]. The most interesting aspect of such a repulsion mechanism is that old or sick cells are distinguished from younger ones by the strong reduction in the flickering amplitude which would render them more sticky.

Acknowledgments.

This work was enabled by a grant from the Deutsche Forschungsgemeinschaft (contract number Sa 246/13-3) and was further supported by the Fonds der Chemischen Industrie and the Leonhard-Lorentz-Stiftung of the TUM. Helpful discussions with Dr. Pfafferott from the Innere Klinik I of the TUM are gratefully acknowledged.

References

[1] BROCHARD, F. and LENNON, J. F., *J. Physique* **36** (1975) 1035.
[2] STOKKE, B. T., MIKKELSEN, A., ELGSAETER, A., *Europ. Biophys. J.* **13** (1986) 203.
[3] FRICKE, K., WIRTHENSOHN, K., LAXHUBER, R. and SACKMANN, E., *Europ. Biophys. J.* **14** (1986) 67.
[4] BRANTON, D., COHEN, C. M., TYLER, J., *Cell* **24** (1981) 24.
[5] EVANS, E. A. and LA CELLE, P. L., *Blood* **43** (1982) 29.
[6] EVANS, E. A., *Biophys. J.* **14** (1974) 923.
[7] WOLFE, J., STEPONKUS, P. L., *Biochim. Biophys. Acta* **643** (1981) 663.
[8] FRICKE, K. and SACKMANN, E., *Biochim. Biophys. Acta* **803** (1984) 145.
[9] EVANS, E. A. and SKALAK, R., *Mechanics and thermodynamics of Biomembranes* (CRC-press Boca Raton) 1980.
[10] HOCHMUTH, R. W., WORTHY, P. R. and EVANS, E. A., *Biophys. J.* **26** (1979) 101.
[11] ENGELHARDT, H., GAUB, H. and SACKMANN, E., *Nature* **307** (1984) 2378.
[12] PETERSEN, N. O., MC CONNAUGHEY, W. B., ELSON, E. L., *Proc. Natl. Acad. Sci. USA* **79** 5327.
[13] SCHNEIDER, M. B., JENKINS, J. T. and WEBB, W. W., *J. Physique* **45** (1985) 1457.
[14] ENGELHARDT, H., DUWE, H.-P. and SACKMANN, E., *J. Phys. Lett.* **46** (1985) 395.
[15] KRAMER, L., *J. Chem. Phys.* **55** (1971) 2097.
[16] PERA, F. and PIPER, I., *Blut* **41** (1980) 377.
[17] BECK, K. and BEREITER-HAHN, J., *Microscopica Acta* **84** (1981) 153.
[18] PATZELT, W. I., *Leitz-Mitt. Wiss. Tech.* **7** (1979) 141.
[19] GINGELL, D. and TODD, I., *Biophys. J.* **26** (1979) 507.
[20] BRUECKMANN, B., THIEME, W., *Appl. Opt.* **24** (1985) 2145.
[21] BRESENHAM, J. F., *IBM Syst. J.* **4** (1965) 25.
[22] EVANS, E. A. and FUNG, Y. C., *Microvasc. Research* **4** (1972) 335.
[23] PAPOULIS, A., *The Fourier Integral and its Applications* (McGraw-Hill) 1962.
[24] HELFRICH, W., Z. *Naturforscher* **339** (1978) 305.
[25] EVANS, E. A. and PARSEGIAN, V. A., *Proc. Natl. Acad. Sci. USA* **83** (1986) 7123.